

Heteroepitaxy of single-crystal LaLuO₃ on GaAs(111)A by atomic layer deposition

Yiqun Liu,¹ Min Xu,² Jaeyeong Heo,¹ Peide D. Ye,² and Roy G. Gordon^{1,a)}

¹Department of Chemistry and Chemical Biology, Harvard University, Cambridge, Massachusetts 02138, USA

²School of Electrical and Computer Engineering and Birck Nanotechnology Center, Purdue University, West Lafayette, Indiana 47907, USA

(Received 6 September 2010; accepted 29 September 2010; published online 21 October 2010)

We demonstrate that LaLuO₃ films can be grown epitaxially on sulfur-passivated GaAs(111)A substrates by atomic layer deposition (ALD). Transmission electron microscopy and x-ray diffraction analyses reveal that the oxide film exhibits a cubic structure with a lattice mismatch of -3.8% relative to GaAs. The epitaxial layer has a high degree of crystalline perfection and is relaxed. Electrical characterizations performed on this structure show interfaces with a low interface state density of $\sim 7 \times 10^{11} \text{ cm}^{-2} \text{ eV}^{-1}$. The measured dielectric constant is around 30, which is close to its bulk crystalline value. In contrast, ALD LaLuO₃ is polycrystalline on GaAs(100) and amorphous on Si(111). © 2010 American Institute of Physics. [doi:10.1063/1.3504254]

Lanthanum lutetium oxide (LaLuO₃) has been widely studied as an alternative gate dielectric to replace silicon dioxide for metal-oxide-semiconductor field-effect transistors (MOSFETs). Single crystals of this oxide have a high dielectric constant ($\kappa \sim 30$) and a large optical band gap (5.6 eV).¹ LaLuO₃ films have been grown by several physical and chemical methods. Epitaxial cubic LaLuO₃ thin films were grown on Si(111) by molecular beam epitaxy (MBE) at 700 °C (Ref. 2) and orthorhombic LaLuO₃ on both SrTiO₃ and SrRuO₃(100) by pulsed-laser deposition at temperatures higher than 600 °C.³ Amorphous films were also made on Si by these techniques at relatively lower temperatures (< 450 °C).^{4–6} We have reported that high-quality amorphous LaLuO₃ thin film grew by atomic layer deposition (ALD) on H-terminated Si(100) at 300 °C and showed promising electrical results.⁷

The aggressive scaling of MOSFETs has created interest in using high mobility III–V channel materials to replace traditional strained Si. However, it has been challenging to form dielectrics that can passivate III–V surfaces with a low interface state density (D_{it}).⁸ Several dielectrics have been investigated. For example, epitaxial cubic Gd₂O₃ ($\kappa \sim 10$) was deposited by MBE to passivate GaAs(100) surfaces and a low D_{it} was obtained.⁹ Epitaxial perovskite SrTiO₃ was grown by MBE on GaAs(100) with sharp interfaces and a high κ but a low D_{it} was not found.¹⁰ However, these deposition techniques are not considered as commercially practical processes. Therefore, many efforts have been made to study oxides such as amorphous Al₂O₃ and HfO₂ on GaAs made by ALD (Refs. 11–13) but the κ values of these materials are relatively low and the structures need lower D_{it} . The work presented here deposits LaLuO₃ dielectrics by ALD on sulfur-passivated GaAs substrates. LaLuO₃ films were grown epitaxially on GaAs(111)A by a low-temperature ALD process. Both high κ and low D_{it} were obtained together by a commercially practical process.

LaLuO₃ thin films were deposited from the precursors including lanthanum tris(*N,N'*-diisopropylformamidinate),

lutetium tris(*N,N'*-diethylformamidinate), and H₂O in a horizontal gas flow reactor. The deposition temperature was fixed at 350 °C. The deposition was done by repeatedly growing one cycle of La₂O₃ followed by one cycle of Lu₂O₃. The metal precursors were delivered with high-purity nitrogen assist. The exposures of the La and Lu precursors were estimated to be around 0.003 Torr s and the exposure of H₂O was about 0.06 Torr s in each cycle. The chamber was purged under nitrogen for 40 s and 60 s after the metal precursor and H₂O pulse, respectively. Such a long purging time minimized the number of hydroxyl groups trapped in the film. N-type GaAs(111)A wafers with carrier concentration around $5 \times 10^{17} \text{ cm}^{-3}$ were used as substrates. GaAs(100) and Si(111) wafers were also studied for comparison. Before deposition, all GaAs substrates were passivated by first dipping into an HCl:H₂O=1:1 solution to remove the native oxide and then soaking in a 20% (NH₄)₂S solution for 10 min at room temperature for S-passivation. Si wafers were dipped in 5% HF solution for 10 s before deposition. The deposition rate was 0.2 nm for a complete cycle of LaLuO₃. The composition ratio of La:Lu was about 1:1 estimated by Rutherford backscattering spectroscopy. For electrical characterizations, all samples were capped with 6 nm ALD-Al₂O₃ and subjected to rapid thermal anneal at 700 °C in N₂ ambient for 30 s. Ni/Au circular electrodes for MOS capacitors were patterned by a lift-off process with a diameter of 150 μm.

Figure 1 shows a cross-sectional transmission electron microscopy (TEM) micrograph of LaLuO₃/GaAs(111)A and the inset corresponds to its in-plane selected area electron diffraction pattern. The magnified image of the interface is shown at the bottom. The sample for cross-sectional TEM image has 12 nm LaLuO₃ deposited on GaAs by 60 complete LaLuO₃ cycles. The electron beam is oriented along the $\langle 110 \rangle$ direction of the GaAs substrate. The oxide is uniform in thickness and is approximately 35 monolayers thick. As shown in Fig. 1, a twin relationship is observed between the oxide and underlying GaAs substrate at the common (1 $\bar{1}\bar{1}$) interface. Similar epitaxial relations were found in (La_xY_{1-x})₂O₃ and (La_xLu_{1-x})₂O₃ (cubic) on silicon (111)

^{a)}Electronic mail: gordon@chemistry.harvard.edu.

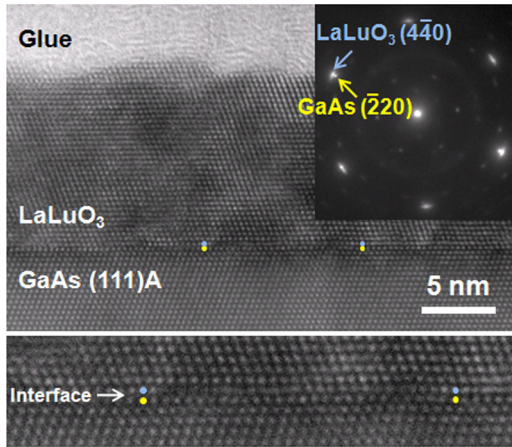


FIG. 1. (Color online) Cross-sectional TEM micrograph of the LaLuO₃/GaAs(111)A heterostructure. The magnified image at the interface is shown at the bottom. The inset shows the selected area diffraction pattern in the 111 pole of the substrate.

grown by MBE.^{2,14} By carefully examining the interface, it is found that a metal atom of LaLuO₃ sits right on top of a lattice point of GaAs every 28 columns (see marks). This shows that despite the lattice mismatch between LaLuO₃ and GaAs, the oxide layer is mostly relaxed. The diffraction pattern was taken from a sample with 45 nm of LaLuO₃ and shows that the arrays of $\langle 440 \rangle$ diffraction spots from LaLuO₃ are nearly superimposed on those $\langle 220 \rangle$ from GaAs. The structure of LaLuO₃ is identified as a cubic phase.

The epitaxial growth of cubic LaLuO₃ film on GaAs(111)A was further confirmed by high-resolution x-ray diffraction (HRXRD) measurements. Figure 2(a) shows the omega-two theta scan for the LaLuO₃ layer on GaAs(111)A. The LaLuO₃(222) reflection is shifted from the GaAs(111) peak by 0.63°. The lattice constant (a_{oxide}) is estimated to be ~ 10.86 Å. For cube-on-cube epitaxy, the resulting mismatch is -3.8% compared to GaAs ($a = 5.65$ Å), where the mismatch is defined as $(a_{\text{oxide}} - 2a)/2a$. This indicates that the epitaxial film is relaxed with no strain, which is consistent with the TEM observation. The well-defined thickness fringes at both sides of the LaLuO₃(222) peak indicate a high degree of crystalline uniformity over a large area. Figure 2(b) shows the omega scan for the LaLuO₃(222) reflection. The full width at half maximum is 16.5 arc sec, where 1 arc sec is $1/3600^\circ$. This value is equal to the value of 16.2 arc sec for the GaAs(111) substrate peak (not shown here), indicating that the quality of the epitaxial ALD-LaLuO₃ layer is comparable to that of the GaAs substrate.

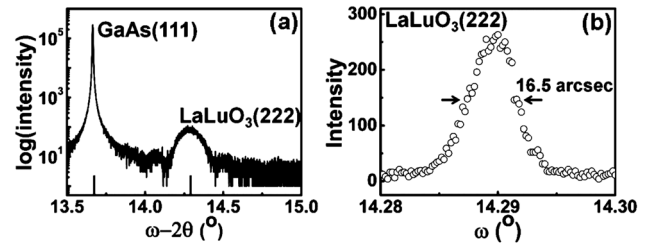


FIG. 2. (a) High-resolution x-ray omega-two theta scan for LaLuO₃ film on GaAs(111)A. (b) The rocking curves of the LaLuO₃(222) peak.

The electrical properties of LaLuO₃/GaAs(111)A were also characterized. Capacitance-voltage (C-V) curves were measured on MOS capacitors with 6 nm Al₂O₃/10 nm LaLuO₃/n-GaAs(111)A stack under different frequencies and temperatures. Since Fermi-level unpinning was reported on ALD Al₂O₃/GaAs(111)A system,¹² a capacitor with 8 nm Al₂O₃/n-GaAs(111)A was measured for comparison. ALD Al₂O₃ was confirmed to be amorphous on GaAs(111)A by cross-sectional TEM studies. As shown in Figs. 3(a) and 3(b), LaLuO₃/GaAs(111)A has a smaller frequency dispersion of 9% on the accumulation side and a smaller flatband shift of 0.2 V between 1 MHz and 1 kHz, compared with 13% and 0.64 V in Al₂O₃/GaAs(111)A. These comparisons indicate that there are fewer electronic defects at the LaLuO₃/GaAs(111)A interface than at the Al₂O₃/GaAs(111)A interface. C-V curves showed little difference among six pads of each capacitor sample and did not change after two months. From the conductance measurement, D_{it} of LaLuO₃/GaAs(111)A was estimated as $\sim 7 \times 10^{11} \text{ cm}^{-2} \text{ eV}^{-1}$, which is an order of magnitude lower than that of Al₂O₃/GaAs(111)A ($\sim 8 \times 10^{12} \text{ cm}^{-2} \text{ eV}^{-1}$), as shown in Fig. 3(c). Another capacitor with amorphous 10 nm LaLuO₃/2 nm Al₂O₃/n-GaAs(111)A stack was prepared to compare the κ values of crystalline and amorphous LaLuO₃, since LaLuO₃ was found to be amorphous with ALD Al₂O₃ underneath. The κ value of crystalline LaLuO₃ was extracted to be 29–30 from the accumulation capacitance at 1 kHz, which is close to the value of LaLuO₃ crystal,¹ while the κ value of amorphous LaLuO₃ was estimated to be 25–26. These results demonstrate that a high-quality epitaxial LaLuO₃ film on GaAs(111)A has superior electrical properties.

In contrast, LaLuO₃ formed as polycrystalline on S-passivated GaAs(100), as can be seen from the cross-sectional TEM image of Fig. 4(a). Electron diffraction and XRD analysis both indicate that the polycrystalline structure

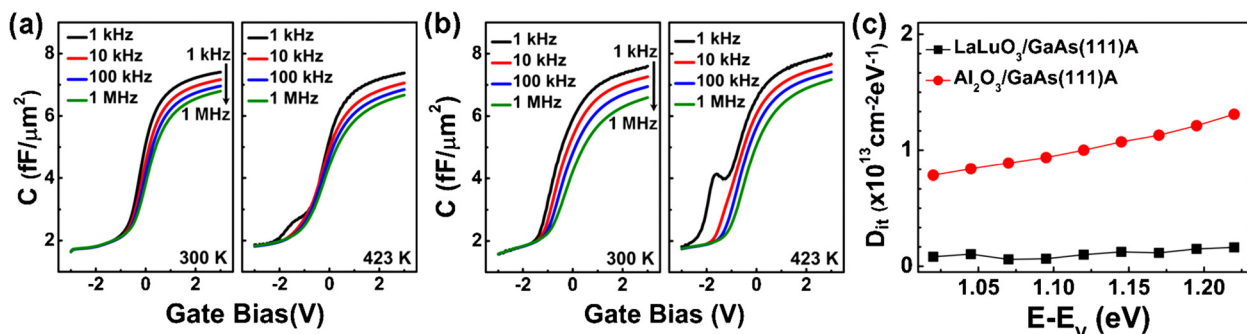


FIG. 3. (Color online) [(a) and (b)] Capacitance-voltage (C-V) characteristics of 6 nm Al₂O₃/10 nm LaLuO₃/n-GaAs(111)A and 8 nm Al₂O₃/n-GaAs(111)A, respectively. (c) D_{it} vs band gap energy.

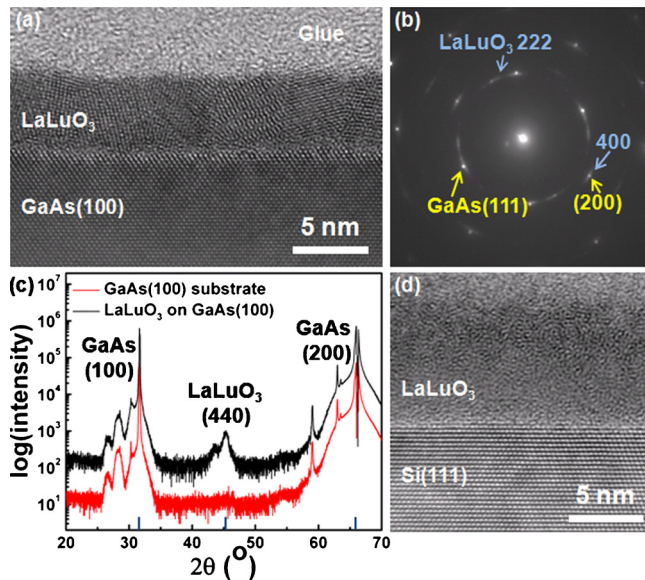


FIG. 4. (Color online) (a) Cross-sectional TEM image of the LaLuO₃/GaAs(100) stack. (b) Electron diffraction pattern on a cross-sectional TEM sample of LaLuO₃/GaAs(100) stack. (c) XRD two theta-omega scan of a LaLuO₃/GaAs(100) sample and a bare GaAs(100) substrate for comparison. (d) Cross-sectional TEM image of the LaLuO₃/Si(111) stack.

is (110) preferentially oriented [Figs. 4(b) and 4(c)]. This orientation can be explained by the model proposed by Yoshimoto *et al.*¹⁵ The model claimed that for oxide epitaxy, the first species to bond with the substrate is oxygen and the growth orientation of the oxide is determined by the spacing between O atoms. In the case of LaLuO₃/GaAs(100), the spacing between the dangling bonds on the GaAs(100) surface is ~ 3.99 Å and the average distance between O atoms in the LaLuO₃(001) plane is ~ 2.72 Å ($\sim 30\%$ mismatch). In the (110) plane the spacings are 3.84 Å ($\sim 3.8\%$ mismatch) and 2.72 Å ($\sim 30\%$ mismatch). Thus better matching is found with the (110) plane, with two possible (110) domain orientations, resulting in a polycrystalline structure with (110) preferential orientation at lower temperatures.^{14,15} This structure is in accord with our observation of polycrystalline LaLuO₃ on GaAs(100). Epitaxy is favored for LaLuO₃/GaAs(111) because the spacing between the dangling bonds on the GaAs(111) surface is ~ 3.99 Å and between O atoms in the (111) plane of LaLuO₃ is ~ 3.84 Å, providing a small mismatch of $\sim 3.8\%$ and one unique domain orientation. Besides, the slow growth rate of ALD-LaLuO₃ can also be an important factor for epitaxy. The rate is estimated as one monolayer for two complete cycles of LaLuO₃ (210 s/cycle). This could provide enough time for adatoms to arrange themselves into their lowest energy configuration and thus form cube-on-cube epitaxy.

Figure 4(d) shows that LaLuO₃ formed an amorphous phase on Si(111), although the substrate has a similar surface configuration with GaAs(111)A and a very small (0.18%) mismatch with LaLuO₃. This finding is explainable by considering the interface reactions between oxide and substrates. Based on enthalpy formation calculations, La₂O₃ and Lu₂O₃ in contact with Si are found to be unstable against silicate

formation.¹⁶ Our previous studies have shown that a very thin silicate layer is formed during the initial growth by using *in situ* Fourier transform infrared spectroscopy.¹⁷ The amorphous interfacial layer disturbs the ordering of Si(111), which leads to random orientation of O atoms. In contrast, the fact that an epitaxial single crystal LaLuO₃ film forms on GaAs(111)A suggests the absence of any amorphous interlayer before initiation of epitaxial oxide growth.

In summary, heteroepitaxial LaLuO₃ on S-passivated GaAs(111)A was achieved by a very low-temperature ALD process. TEM and XRD analyses confirmed that LaLuO₃ has a cubic structure with good crystallinity and no strain in the oxide. Epitaxial LaLuO₃ on n-GaAs(111)A demonstrated well-behaved C-V curves with a low D_{it} of 7×10^{11} eV⁻¹ cm⁻² and a high κ value of 30. Different crystalline structures of LaLuO₃ on GaAs(111)A, GaAs(100), and Si(111) were explained by the spacing of first absorbing oxygen atoms on the substrates. ALD LaLuO₃ could be a promising high- κ candidate for future III-V technology.

Dow Electronic Materials supplied the precursors for lanthanum and lutetium. Some of this work was performed at the Center for Nanoscale Systems (CNS) at Harvard University. Harvard CNS is a member of the National Nanotechnology Infrastructure Network (NNIN). The work at Purdue University is supported by the SRC FCRP MSD Focus Center.

¹D. G. Schlom and J. H. Haeni, MRS Bull. **27**, 198 (2002).

²T. Watahiki, F. Grosse, V. M. Kaganer, A. Proessdorf, and W. Braun, J. Vac. Sci. Technol. B **28**, C3A5 (2010).

³J. Schubert, O. Trithaveesak, W. Zander, M. Roeckerath, T. Heeg, H. Y. Chen, C. L. Jia, P. Meuffels, Y. Jia, and D. G. Schlom, Appl. Phys. A: Mater. Sci. Process. **90**, 577 (2008).

⁴V. V. Afanas'ev, S. Shamuilia, M. Badylevich, A. Stesmans, L. F. Edge, W. Tian, D. G. Schlom, J. M. J. Lopes, M. Roeckerath, and J. Schubert, Microelectron. Eng. **84**, 2278 (2007).

⁵J. M. J. Lopes, M. Roeckerath, T. Heeg, E. Rije, J. Schubert, S. Mantl, V. V. Afanas'ev, S. Shamuilia, A. Stesmans, Y. Jia, and D. G. Schlom, Appl. Phys. Lett. **89**, 222902 (2006).

⁶D. H. Triyoso, D. C. Gilmer, J. Jiang, and R. Droopad, Microelectron. Eng. **85**, 1732 (2008).

⁷H. T. Wang, J. J. Wang, R. Gordon, J. S. M. Lehn, H. Z. Li, D. Hong, and D. V. Shenai, Electrochem. Solid-State Lett. **12**, G13 (2009).

⁸J. Robertson, Appl. Phys. Lett. **94**, 152104 (2009).

⁹M. Hong, J. Kwo, A. R. Kortan, J. P. Mannaerts, and A. M. Sergent, Science **283**, 1897 (1999).

¹⁰Y. Liang, J. Kulik, T. C. Eschrich, R. Droopad, Z. Yu, and P. Maniar, Appl. Phys. Lett. **85**, 1217 (2004).

¹¹N. Goel, P. Majhi, C. O. Chui, W. Tsai, D. Choi, and J. S. Harris, Appl. Phys. Lett. **89**, 163517 (2006).

¹²M. Xu, K. Xu, R. Contreras, M. Milojevic, T. Shen, O. Koybasi, Y. Q. Wu, R. M. Wallace, and P. D. Ye, Tech. Dig. - Int. Electron Devices Meet. **2009**, 865.

¹³M. L. Huang, Y. C. Chang, C. H. Chang, Y. J. Lee, P. Chang, J. Kwo, T. B. Wu, and M. Hong, Appl. Phys. Lett. **87**, 252104 (2005).

¹⁴V. Narayanan, S. Guha, N. A. Bojarczuk, and F. M. Ross, J. Appl. Phys. **93**, 251 (2003).

¹⁵M. Yoshimoto, H. Nagata, T. Tsukahara, and H. Koinuma, Jpn. J. Appl. Phys., Part 2 **29**, L1199 (1990).

¹⁶L. Marsella and V. Fiorentini, Phys. Rev. B **69**, 172103 (2004).

¹⁷J. Kwon, M. Dai, M. D. Halls, E. Langereis, Y. J. Chabal, and R. G. Gordon, J. Phys. Chem. C **113**, 654 (2009).